GEOLOGICAL NOTES

Quaternary Glacial-Interglacial Climate Cycles in Hawaii

Nathan D. Sheldon

Department of Geology, Royal Holloway University of London,
Egham, Surrey TW20 0EX, United Kingdom
(e-mail: n.sheldon@gl.rhul.ac.uk)

ABSTRACT

The upper kilometer of the Hawaiian Scientific Drilling Program core consists of lavas that were emplaced subaerially, burying paleosols. These paleosols were preserved with minimal alteration and are used to construct a ~330-kyr Quaternary climate record. Within the temporal resolution of this record, there appears to be a ~100-kyr climate oscillation between cool-dry and warm-wet conditions, indicating that tropical regions such as Hawaii have responded to the same global climate forcings as have higher-latitude areas during at least the past three glacial-interglacial cycles. It is also suggested that Hawaiian climate may have become progressively warmer and wetter over the same period.

Online enhancements: appendixes.

Introduction

High-resolution records of Quaternary climate change come from a variety of proxy records, including cave calcites (Winograd et al. 1992), benthic foraminifera, ice cores (Petit et al. 1999), and corals (Gallup et al. 2002), but there are comparatively few continuous soil records (e.g., Busacca 1989), except in the Chinese Loess Plateau (Zhisheng et al. 2005). In glaciated regions of North America and Europe, soils tend to form during interglacial periods, with one major soil surface for each warm, wet interval preserved among the glacial sediments. In contrast, tropical soils formed continuously during both glacial and interglacial times (Gavenda 1992), offering the possibility of more complete records of global change.

Sequences of basalt flows often preserve paleosols with minimal alteration (Sheldon 2003). For this reason, Hawaii offers the possibility of a relatively high-resolution terrestrial Quaternary climate record of both glacial and interglacial intervals. The Hawaiian Scientific Drilling Program (HSDP; H-2 core) collected a continuous core to a depth of >3000 m, 1079 m of which were emplaced subaerially (figs. 1, 2; DePaolo et al. 2001). Core recovery was generally good (>95%), though not every soil profile collected is likely complete. Soils formed during times of quiescence in flow emplacement (fig. 1) and have been used to construct a ~330-kyr Quaternary paleoclimate record.

Manuscript received June 16, 2005; accepted November 22, 2005.

Methods

It is not within the scope of this note to discuss the actual collection of the core, but a detailed description may be found in an article by DePaolo et al. (2001). The drill site was located near the Hilo International Airport on the Big Island of Hawaii (lat 19°42′40N, long 155°03′20W; fig. 1). The subaerially emplaced portion of the core (1079 m) consists primarily of tholeiitic and alkalic lavas erupted by Mauna Kea, with the uppermost 254 m consisting of tholeiitic lavas erupted by Mauna Loa (fig. 2).

Core sections were measured and samples collected during January 2002, before the core's move from the California Institute of Technology into a permanent archive at the American Museum of Natural History. Paleosol profiles were identified using observations of horizonation, Munsell color, reaction with dilute acid, and other characteristics,

[The Journal of Geology, 2006, volume 114, p. 367–376] 0022-1376/2006/11403-0007$15.00

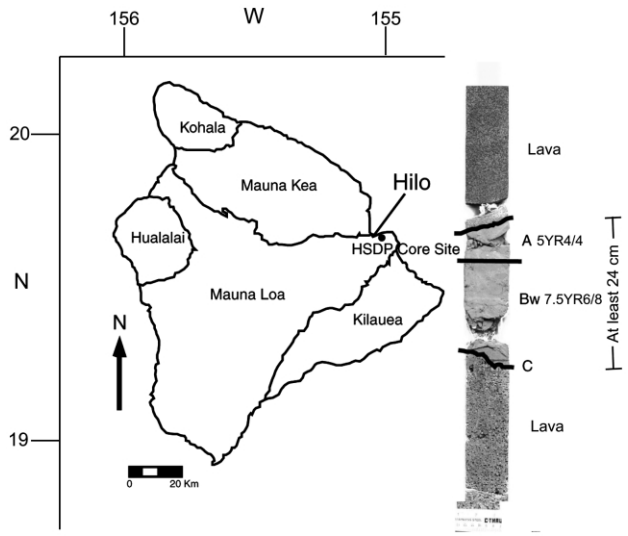

Figure 1. Field map and core photo. The map is modified after DePaolo et al. (2001), and the core photo is of a paleosol at 138.35 m in the Hawaiian Scientific Drilling Program core (DePaolo et al. 1999), with horizons and Munsell colors listed.

including mineral assemblage via petrography (Retallack 1997, 2001). Major and trace elements were analyzed using x-ray fluorescence and inductively coupled plasma mass spectrometry (Bondar Clegg, Vancouver, BC), and data are available in the online edition or from the *Journal of Geology* office.

Isotopic analyses of soil organic carbon were performed by J. Wynn of the University of St. Andrews (then at Australian National University) on samples crushed with mortar and pestle, coarsely sieved (1.25 Φ), and divided into 5-g aliquots. The samples were combusted in quartz tubes at 850°C for 8 h in the presence of excess copper oxide and silver catalyst; CO_2 derived from combustion was cryogenically purified on vacuum extraction lines and measured on a Finnigan MAT 251 with respect to internal standards (ANU sucrose and Fergie sucrose) and reported with respect to the PDB international standard in standard δ notation.

Soil Formation

Description. Paleosols preserved between HSDP core flows are typically light brown (7.5YR6/4) to red (10R4/6) in color without well-defined macro ped structure or bedding (e.g., fig. 1). Most of the paleosols are very low in organic matter or preserve none at all, with exceptions discussed below. The texture of the paleosols is generally granular, though in some cases there are partially rounded, angular shards, consistent with the weathering of volcanic ash (e.g., Retallack et al. 2000; Sheldon 2003). Profiles are thin (<1 m; e.g., app. C), and soil horizonation is typically A-Bw-C, where there is significant reddening of the Bw horizons (fig. 1). Root traces are scarce, millimeter scale, and typically present only in the A horizons or uppermost B horizons. Contacts between paleosols and the underlying basalt flows are gradual and angular, with some illuvial clay among basaltic corestones.

Nonclimatic Soil-Forming Factors. The five primary factors that control soil formation are topography, organisms (vegetation and invertebrates), parent material, time of formation, and climate. The HSDP paleosols formed on fairly flat surfaces, with only microtopography (up to meter scale) provided by the flow top morphology (variation is primarily the result of ′a′a vs. pahoehoe). The fine scale and shallow penetration of root traces in the paleosols indicate that they sustained early successional-type herbaceous vegetation and sparse tree coverage because while some Ohia (*Metrosideros polymorpha*) trees were likely present, no large root traces or taproots were preserved in more than a kilometer of core. There is also no evidence of a burrowing infauna. Parent material is vesicular or massive basalt (mostly) of tholeiitic composition, rarely mantled by more felsic volcanic ash, probably derived from Kilauea (Beeson et al. 1996).

Formation times for the Hawaiian paleosols were relatively short. The lack of large root traces precludes long-lived forest ecosystems that had moved beyond early successional vegetation. Both in hand specimen and in thin sections, there are rounded, weathered, sand-sized olivine grains still present;

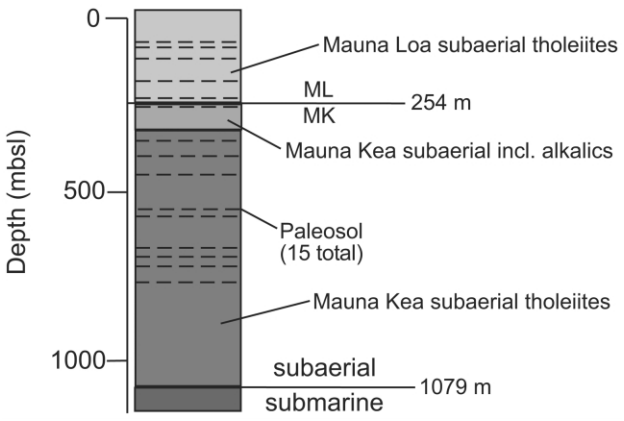

Figure 2. Simplified Hawaiian Scientific Drilling Program core stratigraphy. *ML* = Mauna Loa; *MK* = Mauna Kea.

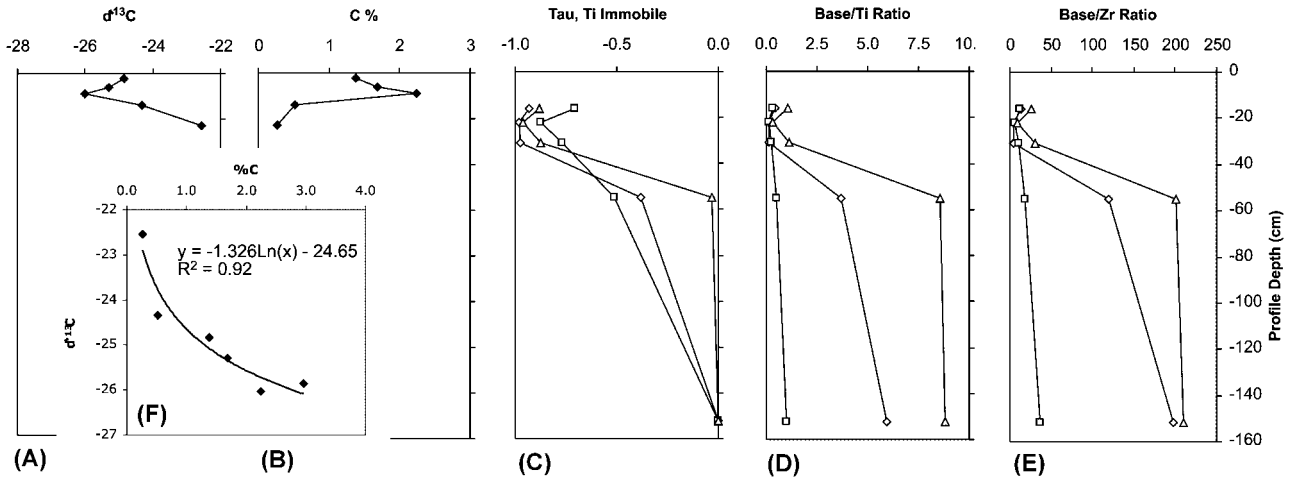

Figure 3. Geochemical profiles for a ~130-ka-old paleosol. Symbols are consistent throughout. *Open squares* = Na; *open triangles* = Mg; *open diamonds* = Ca. Sr, K, and Rb are also plotted in the online edition. Samples H14–H16, H18–H19 (see online edition). A τ value of -1.0 would reflect complete (100%) removal of a given cation, whereas a value of 1.0 would reflect a doubling of the cation (i.e., 100% increase). The relationship between carbon concentration and carbon isotopic composition is consistent with Rayleigh distillation, which predicts a linear or logarithmic relationship (e.g., Wynn et al. 2005).

olivine is typically not very resistant to weathering. Thin profiles and a lack of Bt horizons (well-developed clay-rich horizons) also indicate only moderate weathering. Taken together, these qualitative lines of evidence and comparison with modern soils suggest that the HSDP paleosols formed in hundreds to a few thousand years. This estimate is consistent with accumulation and flow emplacement rates for the core (DePaolo et al. 2001). Further refinement of soil formation times is not presently possible, given the uncertainties of existing dating methods (i.e., K-Ar and Ar-Ar; analytical uncertainty is larger than the time of formation). Using the USDA soil classification scheme, the Hawaiian paleosols are classified as either Inceptisols (weakly to moderately developed soils) or Andisols (soils formed from volcanic ash). In general, the Quaternary paleosols from the HSDP core share many features (horizonation, taxonomic affinity, etc.) with modern Hawaiian soils and paleosols exposed at the surface elsewhere (e.g., Chadwick et al. 1999 and references therein).

Inorganic Geochemistry. During soil formation, alkali (e.g., K, Na, Rb) and alkaline earth (e.g., Ca, Mg, Sr) elements are liberated from the parent material through a combination of leaching and hydrolysis reactions. Other elements such as Ti, Nb, Zr, and Al are immobile or less mobile during weathering. However, in Hawaii, this rule of thumb breaks down for modern soils that receive very high precipitation (>2500 mm mean annual precipitation [MAP]; Kurtz et al. 2000). Molar ratios of mobile to immobile elements are one way of quantifying weathering (fig. 3; app. B). Low ratios in the upper horizons of the paleosols compared with the lower horizons indicate that Ca, Mg, and Sr were leached extensively during soil formation; Na and Rb were leached much more weakly, and there was addition or no net loss of K (see app. B for additional data omitted from fig. 3). These results are similar to Vitousek et al.'s (1997) results from modern Hawaiian soils and recent paleosols. In general, cation loss follows this pattern: $\mathrm{Mg} \approx \mathrm{Ca} > \mathrm{Sr} \gg \mathrm{Na} \approx \mathrm{Rb} > \mathrm{K}$. Rb and K exhibit similar geochemical behavior, so if K had been added by some postburial process, Rb would be expected to have a similar distribution (Sheldon 2003). Because it does not, the very slight accumulation of K is probably because of the short durations of soil formation during which K was not leached as efficiently as more labile cations such as Ca and Mg.

Weathering fluxes can be calculated on the basis of changes in concentration of the cation of interest, as compared with an immobile element. Mass balance calculations were made using standard methods (Chadwick et al. 1990; see app. B). Because of the extremely limited amount of sample available, the density of the samples was not measured but was instead estimated to be 1.32 $\mathrm{g/cm^{-3}}$ for the paleosols (Inceptisols; Sheldon and Retallack 2001)

and 2.7 g/cm^{-3} for the basalt (Sheldon 2003). Ti was nearly immobile during weathering, while other typically immobile cations such as Nb, Zr, and Al (Kurtz et al. 2000) were moderately to very mobile. The A and Bw horizons of the paleosols typically have lost more than 90% of their Ca and Mg and more than 75% of their Na relative to the parental basalt (fig. 3).

Soil Organic Matter. While there is typically little organic matter preserved in the Hawaiian paleosols, some of the paleosols are brownish in color and have retained a significant amount of organic material (>2.4% by mass). Preserved soil organic carbon decreases with depth in the profile below the uppermost part of the Bw horizon (fig. 2). $\delta^{13}C$ values from paleosol organic matter range from −22 to −26‰ in two paleosols, values consistent with C3 photosynthesis (Koch 1998). However, because of the strong correlation between $\delta^{13}C$ values and weight percent of C (fig. 3), it is likely that the $\delta^{13}C$ of the organic matter was enriched by Rayleigh distallation (J. G. Wynn, pers. comm.). The variation in $\delta^{13}C$ values in the profile is thus in part a function of burial rather than solely of original biotic activity. The conclusion that these paleosols supported C3 vegetation is confirmed by palynological data (Gavenda 1992) and the observation that with higher organic matter levels (as in soils before burial), even more depleted $\delta^{13}C$ values would be predicted, consistent with C3 rather than C4 or CAM plants, both of which are characterized by heavier $\delta^{13}C$ values.

Paleoclimatic Reconstruction

The degree of chemical weathering of paleosol Bt and Bw horizons can be related to MAP and mean annual temperature (MAT) using climofunctions derived from a North American soil survey of modern soil bulk-rock geochemistry (Sheldon et al. 2002). The chemical index of alteration without potassium (CIA − K) can be related to MAP as follows:

$$\text{MAP (mm)} = 221.2e^{(.0197\text{CIA}-\text{K})}, \quad (1)$$

where $R^2 = 0.72$, with a standard error of ±182 mm (Sheldon et al. 2002), and

$$\text{CIA} - \text{K} = 100 \times \frac{m\text{Al}_2\text{O}_3}{m\text{Al}_2\text{O}_3 + m\text{CaO} + m\text{Na}_2\text{O}}$$

(Maynard 1992). This function gives paleoprecipitation estimates consistent with other proxies, including the depth to a Bk horizon and from plant leaf-margin analysis (Sheldon et al. 2002), and was recently used to "predict" successfully present-day precipitation values based on modern soils as a reversal test on the viability of the proxy (Driese et al. 2005). A new function derived from the database of Sheldon et al. (2002) for use exclusively with Inceptisols allows MAT to be calculated as follows:

$$\text{MAT (°C)} = 46.94C + 3.99, \quad (2)$$

where $R^2 = 0.96$, with a standard error of 0.6°C, and $C = m\text{Al}_2\text{O}_3/m\text{SiO}_2$. C is a measurement of "clayeyness" in paleosols (Retallack 2001), and modern Hawaiian soils have long been known to show an increased proportion of clay in soils that formed under warmer or wetter local conditions (e.g., Sherman 1952). Most of the results from this new function fall within the standard error of the previously published function for MAT from the same study (and same database), which gives estimates consistent with data from plant fossils (Sheldon et al. 2002). Because these proxies rely only on characteristics of the B horizons of the paleosols, incomplete preservation of paleosol profiles (e.g., partial removal of the A horizon by subsequent lava flows or drill core collection) does not compromise the paleoclimatic estimates.

Age Model. It is possible to construct a simple age-depth model to determine the age of a given paleosol in the core using existing radiometric dates. Sharp et al. (1996) published a number of ages (K-Ar, Ar-Ar) from the pilot hole that preceded the deeper penetration of the HSDP core, but some of those ages are contradictory (i.e., deeper samples with younger ages). The pilot hole also contained clastic materials, such as beach sands (Beeson et al. 1996) and corals (Moore et al. 1996), which are difficult to correlate into the HSDP core, and some of the dated ash layers were actually fall deposits from Kilauea (Beeson et al. 1996). Thus, even though the pilot hole and main HSDP hole were drilled just a few kilometers apart, many of the previously published ages from materials other than basalt are not useful for this study. Instead, new ages on HSDP core basalts have been used (D. DePaolo, pers. comm., 2002; W. Sharp and Berkeley Geochronology Center, unpublished dates) in combination with the earlier basalt ages from the pilot hole, and the following age-depth model was found:

$$\text{age (kyr)} = \frac{728.05 \times D\ \text{(m)}}{766.25 + D\ \text{(m)}}, \quad (3)$$

where D is depth, $R^2 = 0.97$, and the standard error is 35.3 kyr (fig. 4; ages and uncertainties are tab-

ulated in table A4). However, given that stratigraphic superposition is absolute in a basalt-paleosol sequence and that a few of the paleosols are stratigraphically very close to dated basalt flows, the actual uncertainty on the age assignments is smaller than the standard error would suggest; thus, though the absolute age of a given paleosol has some uncertainty, the relative age and sequence of ages has very little. Using the age model, the submarine-subaerial transition at 1079 m would have an age of 426 kyr, an age consistent with previous age estimates based on volcano growth models for the emergence of Mauna Kea above sea level (Moore and Clague 1992).

However, all of the ages used to find this relationship are from Mauna Kea lavas, and the upper 254 m of the core are Mauna Loa lavas. The Mauna Loa lavas represent the main shield-building stage, while the upper Mauna Kea lavas represent the terminal alkalic stage of volcanic growth (DePaolo et al. 2001), so the extrusion rates may have been different. As a result, I have assumed a linear relationship between the age and depth of the terminal Marine Oxygen Isotope Stage 5e (MIS-5e; Petit et al. 1999) paleosol and the surface to determine the age of the Mauna Loa paleosols, where

$$\text{age (kyr)} = 0.5459 \times D \text{ (m)}. \quad (4)$$

A 300-kyr Paleoclimate Record. Reconstructed MAP ranged from ~400 to 1200 mm and MAT from ~11° to 24°C over the ~330-kyr record, and both MAP and MAT show a cyclicity similar to the 100-kyr period dominant in late Quaternary paleoclimatic records (e.g., Petit et al. 1999; fig. 5). Present-day Hilo has an MAT of 23°C and receives >3000 mm MAP (http://www.wrcc.dri.edu; accessed September 17, 2003). Estimated warm and wet conditions in the HSDP record correspond fairly well to high atmospheric CO_2 values (fig. 5) measured from the Vostok ice core (Petit et al. 1999), while cool and dry conditions correspond fairly well to lower atmospheric CO_2 values. In general, there is good correspondence between the paleosol record, CO_2 record, and MIS6–MIS10. The five youngest paleosols are an important exception, showing poor correspondence with isotope and CO_2 records (fig. 5*A*). Those paleosols are all from the undated Mauna Loa portion of the HSDP core, and the "old" ages from equation (3) are likely an artifact of the transition between alkalic emplacement in the late stages of Mauna Kea's growth and tholeiitic emplacement in an earlier stage of Mauna Loa's growth. Given the general correspondence between CO_2 levels and paleoclimatic conditions shown by

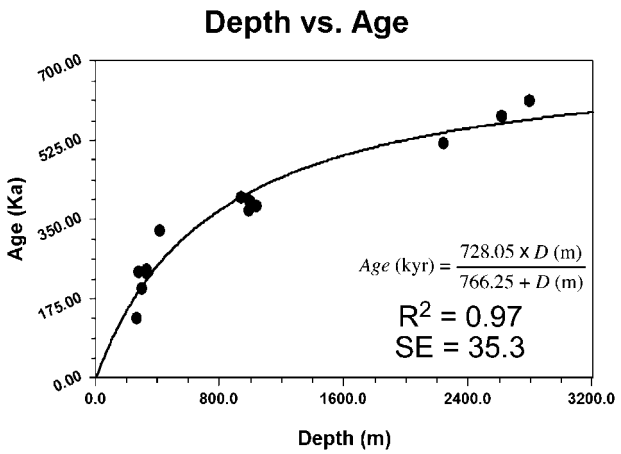

Figure 4. Depth versus age relationship. Construction of the curve as described in the text.

the older paleosols, I have assigned an age of 130 kyr to deepest paleosol within the Mauna Loa lavas and have fit the ages of the younger paleosols linearly using equation (4) (fig. 5*B*). That paleosol records the warmest and wettest conditions of the entire record, consistent with the observation that the 130-kyr (MIS-5e) interglacial was the warmest of the Quaternary before the present one (Winograd et al. 1992; Petit et al. 1999), lending further support to that age assignment. Furthermore, Sharp et al. (1996) obtained an age of 132 ± 32 kyr for the basal Mauna Loa flow in the trial hole at a depth of 268 m, while the proposed MIS-5e paleosol is at a depth of 238 m. That chronostratigraphic relationship fits considerably better with the age model used in figure 5*B* than the one in figure 5*A* and results in a reasonable correspondence between the paleosol record and both the CO_2 and isotope records for MIS3–MIS10. Without further targeted dating of the Mauna Loa lavas, it is not possible to improve the chronology of the uppermost paleosols.

Discussion

Burial Processes and Postburial Alteration. As discussed in "Inorganic Geochemistry," the distribution of alkali elements (K and Rb) in the paleosol profiles is consistent with a weathering rather than a metasomatic/baking origin (e.g., Sheldon 2003). Other evidence of baking such as zeolitization or ceramicization of paleosol clays was similarly absent.

Another type of alteration that needs to be considered is degassing by the volcanic system into the overlying soils. Stephens and Hering (2002) describe

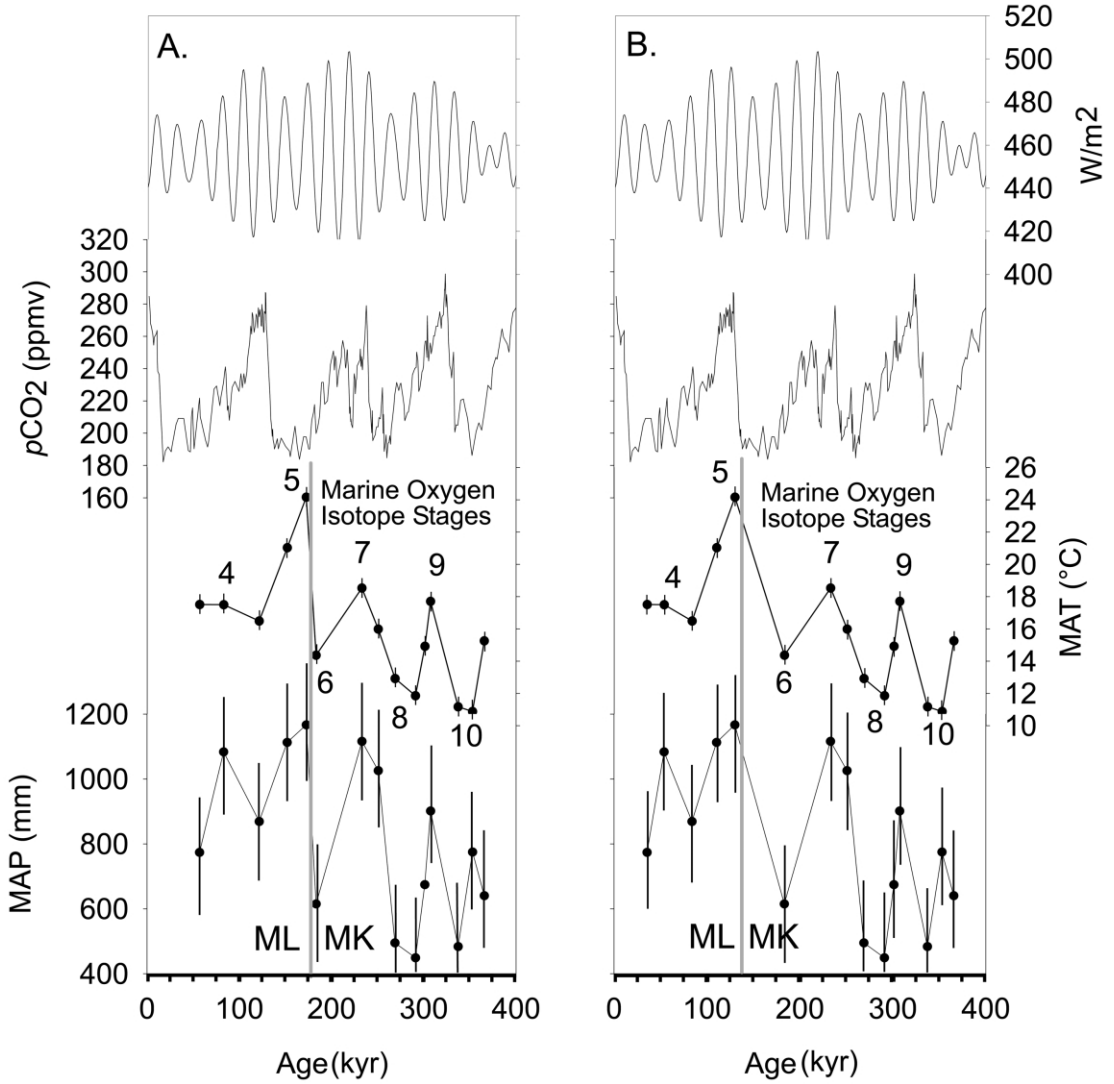

Figure 5. Mean annual precipitation and mean annual temperature for Hilo compared with insolation and atmospheric pCO_2 over the past 400 ka. *ML* = Mauna Loa lavas; *MK* = Mauna Kea lavas. *A*, Ages derived using equation (3). *B*, Corrected ages derived using equation (3) for Mauna Kea lavas and equation (4) for Mauna Loa lavas. Insolation data are from Berger and Loutre (1991) and are for 15°N. Atmospheric pCO_2 values are from the Vostok ice core (Petit et al. 1999).

such a system at Mammoth Mountain, California, and note three characteristics that may be useful to assess whether a similar situation prevailed here: (1) a tree "kill zone," (2) soils depleted in Al (because of low soil pH), and (3) soils enriched in Si. While it is difficult to assess the presence of a tree kill zone on the basis of the materials available from a single small-diameter hole, mass balance calculations may be used to assess gains/losses of Si and Al (see table A3). Average τ_{Al} from three profiles range from −0.17 to 0.02 (mean = −0.07), indicating virtually no change in Al. In contrast, average τ_{Si} values from the same three profiles range from 0.03 to −0.59 (mean = −0.36), indicating significant Si mobility, a pattern consistent with pedogenesis. These trends are the opposite of those predicted for soils that had been subjected to repeated long-term volcanic degassing; thus, this possibility is discounted.

In contrast, Rayleigh distillation of the soil organic matter, evidenced in part by the correlation between weight percent C and the $\delta^{13}C$ value of the individual samples, appears to have played a role in slightly modifying the observed results. Though

literature on the phenomenon is somewhat limited, Wynn et al. (2005) examined $\delta^{13}C$ depth profiles of modern soils and found preferential Rayleigh distillation (enhanced $\delta^{13}C$) of finer-grained soils (~5‰) relative to more coarsely grained soils (~1‰) if all other soil-forming factors (climate, vegetation, topography, time) are the same. The Rayleigh distillation also equilibrated at a greater depth in fine-grained soils, a pattern repeated here (fig. 3). The enhancement of $\delta^{13}C$ with depth of ~2‰–2.5‰ (fig. 3) is consistent with grain/ped sizes intermediate to the two end members of Wynn et al. (2005) and with a moderately mature mixed-grain-size soil. Thus, in combination with textural observations ("Description"), this implies that the distribution of the organic matter in these paleosols is consistent with pedogenesis (i.e., natural burial processes including oxidation) rather than postburial alteration such as metasomatism.

Overall, then, there appears to have been little significant postburial alteration of the HSDP paleosols. Though the emplacement of subsequent basalt flows may have caused some minor alteration of the paleosols, the chemical composition of these paleosols can clearly be attributed to pedogenic rather than postburial processes.

Relating Chemical Weathering and Climate. Modern Hawaiian soils (e.g., Vitousek et al. 1997; Chadwick et al. 1999, 2003; Kurtz et al. 2000) and the weathering of basalt in general (e.g., Chadwick and Chorover 2001; Dessert et al. 2003; Das et al. 2005) have been much studied. While there are some obvious differences between these paleosols (e.g., loss of most of the original organic matter in the paleosols) and many of those modern soils, there are some generalities that have emerged from that body of work that are useful here. For example, Kurtz et al. (2000) found τ_{Al} values of roughly −0.6 for modern soils in Hawaii that receive ~2500 mm/yr MAP. This value represents significantly more Al loss than for these paleosols. One possible explanation of this is that a pedogenic threshold (e.g., Chadwick and Chorover 2001) has been crossed in the modern soils that was not crossed during the formation of the paleosols. Chadwick et al. (2003) found that among Hawaiian soils with otherwise similar soil formation factors, there appears to be a critical threshold at ~1400 mm/yr MAP; soils receiving more than 1400 mm/yr lost their buffering capacity, had much lower pH values, and were much more leached. The reconstructed MAP of these paleosols is <1200 mm/yr, below the modern pedogenic threshold where buffering capacity during pedogenesis is lost. Thus, the limited mobility of Al in the HSDP paleosols further supports the notion that paleoclimatic conditions, at least locally, were more arid than present conditions. Furthermore, in modern soils above the critical MAP threshold, Si was also extensively leached, whereas below that threshold, τ_{Si} was between −0.2 and −0.4 (Chadwick et al. 2003), a range that includes the mean value of −0.36 found for the HSDP paleosols. Again, the modern relationship appears to hold for the HSDP paleosols, lending further support to the paleoclimatic reconstruction described herein.

Quaternary Climate Change Near Hilo, Hawaii. While the absolute range of reconstructed MAT values is very large (~11°–24°C), the real variability was unlikely to have been of that magnitude. Because of the short formation times of the paleosols, during interglacial periods when water availability may have been limited, cooler temperatures are probably underestimated (i.e., are too low). Reconstructed MAP values are somewhat lower than at present, an effect attributable either to the short formation times of the paleosols (insufficient time to reach chemical equilibrium) or to changing orographic conditions on Hawaii as a result of the accelerated main growth phase of Mauna Loa and the initiation of Kilauea during the period of the record. The overall paleoclimatic picture is consistent with palynological data (e.g., Gavenda 1992) and the $\delta^{13}C$ results from the paleosol organic matter. Both indicate C3 plants rather than C4 (typically grasses) or CAM plants (typically succulents), which would more typically be associated with semiarid environments.

Another potential complicating factor is the presence of glaciers on Mauna Kea during the cold phase of Quaternary climatic cycles. Numerous tills have been identified and mapped (Wolfe et al. 1997) on Mauna Kea, and it is the only Hawaiian volcano with unequivocal glacial features (Porter 1979). Reconstruction of the ice cap suggests it was 10 km in diameter and asymmetrically extended farther downslope to the southeast (toward Hilo) than in other directions (Porter 2005). Subsidence-corrected snowline reconstruction of equilibrium-line altitudes (ELA; equilibrium point between accumulation and melting) suggests that during MIS4 and MIS6, the paleo-snowline would have been at least 1000 m lower than at present, well below the summit (Porter 2005). These ELA depression events correspond to relatively cool and dry climatic shifts in the paleosol record (fig. 5*B*) and may have been responsible for the observed aridification near Hilo, as more potential precipitation was trapped upslope and fell as snow onto the glacier rather than as rain farther downslope. This suggests that in addition

to the overall orographic rain shadow effect of Mauna Kea, some of the variation in the paleoclimatic record may be due to microclimate variations in response to a growing and receding icecap. Meta-analysis of tropical ELAs during the last glacial maximum shows that the scale of ELA change is most pronounced in relatively low-altitude mountain glaciers as on Mauna Kea (cf. Himalayas; Mark et al. 2005). Thus, while the cool temperatures in the paleosol record may have been slightly underestimated, independent reconstructions of paleotemperatures in tropical lowland areas using pollen (Farrera et al. 1999) are consistent with predicted temperature changes from ELA changes (Mark et al. 2005) and may indicate that temperature change really was as large as the paleo-MAT predictions in figure 5*B*.

Climatic conditions on Hawaii appear to have become progressively warmer and somewhat wetter during the past three glacial/interglacial cycles (fig. 5), a pattern that holds up for both the glacial and interglacial intervals. While this effect could be due in part to the changing orography of the Big Island (i.e., subsidence of Mauna Kea), independent evidence suggests that the most recent interglacial before the present one was the warmest of the entire Quaternary (Winograd et al. 1992; Petit et al. 1999). Instead, this change could be due to a variety of factors both intrinsic (e.g., methane; Petit et al. 1999) and extrinsic (e.g., solar magnetic activity; Sharma 2002) to the Earth's climate system. Cool-dry glacial minima are clearly distinguishable from warm-wet interglacials (fig. 5) and, given the uncertainty in age model all of the peaks (and most troughs), can be correlated to global climatic records, though it is impossible to determine whether the peaks in this record lead, lagged behind, or were exactly contemporaneous with the global records.

Global Records of Quaternary Climatic Change. Quaternary glacial/interglacial climate change has been characterized by long slow declines to cold conditions punctuated by rapid shifts to warm conditions dominated by a roughly 100-kyr period. These climatic changes have been widely attributed to changes in the amount of insolation reaching the Earth's surface (the Milankovitch hypothesis; Berger and Loutre 1991). However, the 100-kyr eccentricity cycle varies between 95 and 125 kyr (Berger and Loutre 1991), and the radiation changes are much too small to produce the extreme climatic shifts that have been observed. As a result, most explanations of Quaternary climate change invoke amplification of the 100-ka eccentricity cycle by ice-albedo feedback or as atmospheric CO_2 (Shackleton 2000). These explanations have been challenged by climatic records from cave calcite (Devil's Hole; Winograd et al. 1992) tropical corals (Gallup et al. 2002), foraminifera-based sea-surface temperatures from alkenones (Herbert et al. 2001), and U-Th dating (Henderson and Slowey 2000), which all indicate that the penultimate interglacial period did not occur at the time predicted by the Milankovitch hypothesis. Further, direct measurements made on the Vostok ice core show that the 100-kyr ice-age cycle lags temperature, carbon dioxide, and orbital eccentricity (Shackleton 2000). Without additional dating of Mauna Loa lavas, it is not possible to address directly this question of Quaternary forcing mechanisms with the HSDP paleosol record, and even then, the temporal resolution of a soil record is unlikely to match the precision of many of the other proxy records. However, given the roughly 100-kyr cyclicity in the paleosol record and general correspondence to atmospheric CO_2 levels and marine oxygen isotope stages, the HSDP paleosol record appears to be responding to the same forcings as other Quaternary paleoclimatic proxies. This suggests that high-resolution paleosol records of paleoclimatic and paleoenvironmental change are faithful recorders of those changes and a powerful proxy record and that for at least the past three glacial-interglacial climate cycles, tropical areas such as Hawaii have been responding similarly to higher-latitude areas.

Conclusions

Paleosols from the HSDP core, though formed over relatively short intervals, show significant evidence of pedogenesis during glacial and interglacial times both in terms of their physical (e.g., horizonation) and geochemical (e.g., fig. 3) characteristics. The geochemical composition of the paleosol B horizons was used to reconstruct paleotemperature and paleoprecipitation conditions at the time of their formation. Paleotemperature varied from ~11° to 24°C, and paleoprecipitation varied from ~400 to 1200 mm/yr, with both proxy records exhibiting a ~100-kyr cyclicity consistent with other proxies of Quaternary paleoclimatic conditions from non-tropical settings and long-term trends toward warmer and wetter conditions over the past three glacial/interglacial cycles.

ACKNOWLEDGMENTS

I would like to acknowledge support from Geological Society of America (Harold T. Stearns Fellowship) and the help of C. Seaman in accessing the HSDP core. J. Wynn performed the isotopic anal-

yses, provided helpful discussion of their interpretation, and read an earlier draft of this manuscript. This article has benefited from reviews of an earlier version by P. J. Bartlein and P. McCarthy and from reviews of this version by S. Porter and two anonymous reviewers.

REFERENCES CITED

Beeson, M. H.; Clague, D. A.; and Lockwood, J. P. 1996. Origin and depositional environment of clastic deposits in the Hilo drill hole, Hawaii. J. Geophys. Res. 101:11,617–11,629.

Berger, A., and Loutre, M. F. 1991. Insolation values for the climate of the last 10 million years. Quat. Sci. Rev. 101:297–317.

Busacca, A. J. 1989. Long Quaternary record in eastern Washington, U.S.A., interpreted from multiple buried paleosols in loess. Geoderma 45:105–122.

Chadwick, O. A.; Brimhall, G. H.; and Hendricks, D. M. 1990. From a black to a gray box: a mass balance interpretation of pedogenesis. Geomorphology 3:369–390.

Chadwick, O. A., and Chorover, J. 2001. The chemistry of pedogenic thresholds. Geoderma 100:321–353.

Chadwick, O. A.; Derry, L. A.; Vitousek, P. M.; Huebert, B. J.; and Hedin, L. O. 1999. Changing sources of nutrients during 4 million years of ecosystem development. Nature 397:491–497.

Chadwick, O. A.; Gavenda, R. T.; Kelly, E. F.; Ziegler, K.; Olson, C. G.; Elliott, W. C.; and Henricks, D. M. 2003. The impact of climate on the biogeochemical functioning of volcanic soils. Chem. Geol. 202:195–223.

Das, A.; Krishnaswami, S.; Sarin, M. M.; and Pande, K. 2005. Chemical weathering in the Krishna Basin and Western Ghats of the Deccan Traps, India: rates of basalt weathering and their controls. Geochim. Cosmochim. Acta 69:2067–2084.

DePaolo, D. J.; Stolper, E.; and Thomas, D. M. 2001. Deep drilling into a Hawaiian volcano. EOS: Trans. Am. Geophys. Union 82:149,154–149,155.

DePaolo, D. J.; Stolper, E.; Thomas, D. M.; and Garcia, M. O. 1999. Hawaii Scientific Drilling Project core logs and summarizing data. Two-disc CD-ROM database available from the authors.

Dessert, C.; Dupre, B.; Gaillardet, J.; Francois, L. M.; and Allegre, C. J. 2003. Basalt weathering laws and the impact of basalt weathering on the global carbon cycle. Chem. Geol. 202:257–273.

Driese, S. G.; Nordt, L. C.; Lynn, W.; Stiles, C. A.; Mora, C. I.; and Wilding, L. P. 2005. Distinguishing climate in the soil record using chemical trends in a Vertisol climosequence from the Texas Coastal Prairie, and application to interpreting Paleozoic paleosols in the Appalachian Basin. J. Sediment. Res. 75:340–353.

Farrera, I.; Harrison, S. P.; Prentice, I. C.; Ramstein, G.; Guiot, J.; Bartlein, P. J.; Bonnefille, R.; et al. 1999. Tropical climates at the last glacial maximum: a new synthesis of terrestrial palaeoclimate data. I. Vegetation, lake-levels, and geochemistry. Clim. Dyn. 15: 823–856.

Gallup, C. D.; Cheng, H.; Taylor, F. W.; and Edwards, R. L. 2002. Direct determination of the timing of sea level change during Termination II. Science 295:310–313.

Gavenda, R. T. 1992. Hawaiian Quaternary paleoenvironments: a review of geological, pedological, and botanical evidence. Pac. Sci. 46:295–307.

Henderson, G. M., and Slowey, N. C. 2000. Evidence from U-Th dating against Northern Hemisphere forcing of the penultimate deglaciation. Nature 404:61–66.

Herbert, T. D.; Schuffert, J. D.; Andreasen, D.; Heusser, L.; Lyle, M.; Mix, A.; Ravelo, A. C.; Stott, L. D.; and Herguera, J. C. 2001. Collapse of the California Current during glacial maxima linked to climate change on land. Science 293:71–76.

Koch, P. L. 1998. Isotopic reconstruction of past continental environments. Annu. Rev. Earth Planet. Sci. 26:573–613.

Kurtz, A. C.; Derry, L. A.; Chadwick, O. A.; and Alfano, M. J. 2000. Refractory element mobility in volcanic soils. Geology 28:683–686.

Mark., B. G.; Harrison, S. P.; Spessa, A.; New, M.; Evans, D. J. A.; and Helmens, K. F. 2005. Tropical snowline changes at the last glacial maximum: a global assessment. Quat. Int. 138/139:168–201.

Maynard, J. B. 1992. Chemistry of modern soils as a guide to interpreting Precambiran paleosols. J. Geol. 100: 279–289.

Moore, J. G., and Clague, D. A. 1992. Volcano growth and evolution of the island of Hawaii. Geol. Soc. Am. Bull. 104:1471–1484.

Moore, J. G.; Ingram, B. L.; Ludwig, K. R.; and Clague, D. A. 1996. Coral ages and island subsidence, Hilo drill hole. J. Geophys. Res. 101:11,599–11,605.

Petit, J. R.; Jouzel, J.; Raynaud, D.; Barkov, N. I.; Barnola, J.-M.; Basile, I.; Benders, M.; et al. 1999. Climate and atmospheric history of the past 420,000 years from the Vostok ice core, Antarctica. Nature 399:429–436.

Porter, S. C. 1979. Quaternary stratigraphy and chronology of Mauna Kea, Hawaii: a 380,000-yr record of mid-Pacific volcanism and ice-cap glaciation. I, II. Geol. Soc. Am. Bull. 90:609–611, 980–1093.

———. 2005. Pleistocene snowlines and glaciation of the Hawaiian Islands. Quat. Int. 138/139:118–128.

Retallack, G. J. 1997. A colour guide to paleosols. Chichester, Wiley, 175 p.

———. 2001. Soils of the past: an introduction to paleopedology (2nd ed). London, Blackwell Science, 404 p.

Retallack, G. J.; Bestland, E. A.; and Fremd, T. J. 2000. Eocene and Oligocene paleosols in central Oregon. Geol. Soc. Am. Spec. Pap. 344:1–192.

Shackleton, N. J. 2000. The 100,000-year ice-age cycle identified and found to lag temperature, carbon di-

oxide, and orbital eccentricity. Science 289:1897–1901.
Sharma, M. 2002. Variations in solar magnetic activity during the last 200,000 years: is there a sun-climate connection? Earth Planet. Sci. Lett. 199:459–472.
Sharp, W. D.; Turrin, B. D.; Renne, P. R.; and Lanphere, M. A. 1996. The $^{40}Ar/^{39}Ar$ and K/Ar dating of lavas from the Hilo 1-km core hole, Hawaii Scientific Drilling Project. J. Geophys. Res. 101:11,607–11,616.
Sheldon, N. D. 2003. Pedogenesis and geochemical alteration of the Picture Gorge subgroup, Columbia River basalt, Oregon. Geol. Soc. Am. Bull. 115:1377–1387.
Sheldon, N. D., and Retallack, G. J. 2001. Equation for compaction of paleosols due to burial. Geology 29: 247–250.
Sheldon, N. D.; Retallack, G. J.; and Tanaka, S. 2002. Geochemical climofunctions from North American soils and application to paleosols across the Eocene-Oligocene boundary in Oregon. J. Geol. 110:687–696.
Sherman, B. D. 1952. The genesis and morphology of alumina-rich laterite clays. *In* Fredericksen, A. F., ed. Problems in clay and laterite genesis. New York, Am. Inst. Min. Metal. Eng., p. 154–161.
Stephens, J. C., and Hering, J. G. 2002. Comparative characterization of volcanic soils exposed to decade-long elevated carbon dioxide concentrations at Mammoth Mountain, California. Chem. Geol. 186:301–313.
Vitousek, P. M.; Chadwick, O. A.; Crews, T. E.; Fownes, J. H.; and Hendricks, D. M. 1997. Soil and ecosystem development across the Hawaiian Islands. GSA Today 7:1–8.
Winograd, I. J.; Coplen, T. B.; Landvehr, J. M.; Riggs, A. C.; Ludvig, K. R.; Szabo, B. J.; Kolesc, P. T.; and Revesz, K. M. 1992. Continuous 500,000-year climate record from vein calcite in Devils Hole, Nevada. Science 258: 255–260.
Wolfe, E. W.; Wise, W. S.; and Dalrymple, G. B. 1997. The geology and petrology of Mauna Kea Volcano, Hawaii: a study of postshield volcanism. U.S. Geol. Surv. Prof. Pap. 1557, 129 p.
Wynn, J. G.; Bird, M. I.; and Wong, V. N. L. 2005. Rayleigh distillation and the depth profile of $^{13}C/^{12}C$ ratios of soil organic carbon from soils of disparate texture in Iron Range National Park, Far North Queensland, Australia. Geochim. Cosmochim. Acta 69:1963–1973.
Zhisheng, A.; Youngsong, H.; Weiguo, L.; Zhengtang, G.; Clemens, S.; Li, L.; Prell, W.; et al. 2005. Multiple expansions of C4 plant biomass in East Asia since 7 Ma coupled with strengthened monsoon circulation. Geology 33:705–708.